RESEARCH ARTICLE

ENVIRONMENTAL MICROBIOLOGY | Applied Microbiology International

Denitrification fractionates N and O isotopes of nitrate following a ratio independent of carbon sources in freshwaters

Shengjie Li[1,2] | Zhongxin Luo[1,3,4] | Shuo Wang[1] | Qiong Nan[5] |
Guodong Ji[1]

[1]Key Laboratory of Water and Sediment Sciences, Ministry of Education, Department of Environmental Engineering, Peking University, Beijing, China

[2]Department of Biogeochemistry, Max Planck Institute for Marine Microbiology, Bremen, Germany

[3]China Institute of Water Resources and Hydropower Research, Beijing, China

[4]National Research Center for Sustainable Hydropower Development, Beijing, China

[5]Institute of Environment Pollution Control and Treatment, College of Environment and Resource Science, Zhejiang University, Hangzhou, China

Correspondence
Guodong Ji, Key Laboratory of Water and Sediment Sciences, Ministry of Education, Department of Environmental Engineering, Peking University, Beijing 100871, China.
Email: jiguodong@pku.edu.cn

Abstract
The stable isotope technique has been used in tracking nitrogen cycling processes, but the isotopic characteristics are influenced by environmental conditions. To better understand the variability of nitrate isotopes in nature, we investigated the influence of organic carbon sources on isotope fractionation characteristics during microbial denitrification. Denitrifying cultures were inoculated with freshwater samples and enriched with five forms of organic compounds, that is, acetate, citrate, glucose, cellobiose, and leucine. Though the isotope enrichment factors of nitrogen and oxygen ($^{15}\varepsilon$ and $^{18}\varepsilon$) changed with carbon sources, $^{18}\varepsilon/^{15}\varepsilon$ always followed a proportionality near 1. Genome-centred metagenomics revealed the enrichment of a few populations, such as *Pseudomonas*, *Enterobacter*, and *Atlantibacter*, most of which contained both NapA- and NarG-type nitrate reductases. Metatranscriptome showed that both NapA and NarG were expressed but to different extents in the enrichments. Furthermore, isotopic data collected from a deep reservoir was analysed. The results showed δ^{18}O- and δ^{15}N-nitrate did not correlate in the surface water where nitrification was active, but $^{18}\varepsilon/^{15}\varepsilon$ followed a proportionality of 1.05 ± 011 in deeper waters (≥ 12 m) where denitrification controlled the nitrate isotope. The independence of $^{18}\varepsilon/^{15}\varepsilon$ from carbon sources provides an opportunity to determine heterotrophic denitrification and helps the interpretation of nitrate isotopes in freshwaters.

INTRODUCTION

Nitrogen (N) is an essential nutrient for biological production and is linked intimately to carbon efflux in aquatic environments (Gruber & Galloway, 2008). In recent decades, the N concentration in the biosphere has doubled as a result of anthropogenic pressures (Fowler et al., 2013; Robertson & Vitousek, 2009), posing a great threat to the health of ecosystems and human beings. The availability of N is controlled by several microbially mediated processes in freshwaters (Canfield et al., 2010). Atmospheric dinitrogen is fixed by diazotrophs to produce dissolved ammonium, which

is further converted to nitrate by nitrifying microorganisms. Denitrifying microorganisms reduce nitrate to nitrogen gas, with organic carbon as a common electron donor. As the mitigation of N pollution is the priority of environmental and health agencies worldwide, monitoring N concentrations, input sources, and biogeochemical transformations become important tasks for freshwater management.

To this end, the measure of stable isotope compositions of nitrogenous substances provides a complementary, non-disruptive, and integrative tool for evaluating N sources and investigating N cycling processes across different spatial and temporal scales

(Robinson, 2001). Nitrogen fixation does not declare a strong $\delta^{15}N$ fractionation effect—$\delta^{15}N$ of newly fixed N is around -1‰ (with $\delta^{15}N$ of atmospheric dinitrogen defined to be 0‰) and this isotopic value is invariant with environmental parameters (Bauersachs et al., 2009; Carpenter et al., 1997; Macko et al., 1987; Minagawa & Wada, 1986). In contrast, nitrification and denitrification imprint evident fractionation effects on $\delta^{14}N$ versus $\delta^{15}N$ and $\delta^{16}O$ versus $\delta^{18}O$ of dissolved nitrogen compounds (Asamoto et al., 2021; Buchwald & Casciotti, 2010; Casciotti, 2009; Frey et al., 2014; Granger et al., 2008; Granger & Wankel, 2016; Martin & Casciotti, 2016; Treibergs & Granger, 2017; Wunderlich et al., 2012). Microbial nitrate reduction is the first step of denitrification. It is catalysed by two nitrate reductases—the periplasmic nitrate reductase Nap system with NapA as the catalytic subunit, and the cytoplasmic nitrate reductase Nar system with NarG as the catalytic subunit (Richardson et al., 2001). Though the fractionation factors of N ($^{15}\varepsilon$) and oxygen ($^{18}\varepsilon$) respectively change from environment to environment, a generally accepted paradigm is that $\delta^{18}O$-/$\delta^{15}N$-nitrate follows a certain ratio during nitrate reduction (Asamoto et al., 2021; Frey et al., 2014; Granger et al., 2008; Martin & Casciotti, 2016; Treibergs & Granger, 2017; Wunderlich et al., 2012), which could be used as an indication of denitrification in field research (Carrey et al., 2021; Fang et al., 2015; Fenech et al., 2012; Paredes et al., 2020; Torres-Martinez et al., 2020; Yi et al., 2017).

However, the problem is far from being solved—the pattern in nature might not be similar to what we observed in the laboratory, where model organisms are mostly used to obtain isotope values. A challenging issue in this approach is that various environmental factors influence the selection of enzymes, which impart distinct isotopic values (Li, Wang, Pang, & Ji, 2022). For example, previous studies showed NapA fractionated $\delta^{18}O$ and $\delta^{15}N$ with a $^{18}\varepsilon/^{15}\varepsilon$ ratio near 0.5, while NarG fractionated $\delta^{18}O$ and $\delta^{15}N$ with a ratio near 1.0 (Asamoto et al., 2021; Frey et al., 2014; Granger et al., 2008; Treibergs & Granger, 2017). Together with the change in nitrate isotopes from different sources (e.g., $\delta^{18}O$-nitrate from precipitation and fertilizer are different; Xue et al., 2009), the pattern observed at the ecosystem level becomes complicated and hard to explain with data collected from isolated strains. This obscures the prediction of N processes. To evaluate the variability of isotope effects induced by environmental conditions, our study aims to reveal the effect of carbon sources. Organic carbon substrates vary between different denitrifying environments and might be a critical parameter in determining isotope fractionation effects. A previous study indeed compared isotopes influenced by acetate, benzoate, and toluene in two denitrifying strains, *Thauera aromatica* and *Aromatoleum aromaticum* strain EbN1

(Wunderlich et al., 2012). The results showed a variance in $^{15}\varepsilon$ and $^{18}\varepsilon$, but the $\delta^{18}O/\delta^{15}N$ ratio remained unchanged (near 1.0) (Wunderlich et al., 2012). Nevertheless, the experiment was conducted with pure cultures, which used the same enzyme throughout the denitrification process. As carbon sources manipulate the selection of specific microbial populations which use different nitrate reductases (Carlson et al., 2020; Flynn et al., 2017; Goldfarb et al., 2011; Goldford et al., 2018; Wawrik et al., 2005), carbon sources may also influence nitrate isotopes in an ecosystem, but the controlling mechanisms remain unknown.

To better understand the variability of $\delta^{15}N$- and $\delta^{18}O$-nitrate in freshwaters, this study investigated the influence of carbon sources on isotopes during heterotrophic denitrification. We hypothesised that selective carbon sources would induce different N and O isotope fractionation characteristics by selecting different microorganisms and enzymes. We first obtained five denitrifying cultures, which were enriched with five different organic compounds, as reported in a previous study (Li, Wang, & Ji, 2022). N and O isotope fractionation characteristics during nitrate reduction were examined in each enrichment. Microorganisms and nitrate reductases were investigated with genome-resolved metagenomics and metatranscriptomics. Furthermore, 66 isotope samples collected from a deep reservoir were analysed and matched to the pattern observed in the enrichments. The results elucidate an accurate signal in determining the first step of microbial denitrification and help towards a better understanding and interpretation of N isotope records in freshwater ecosystems.

EXPERIMENTAL PROCEDURES

Culturing

Five denitrifying enrichments were built up and inoculated with sediments collected from Hongze Lake, China ($33°13'26''$, $118°25'40''$ E), as previously reported (Li, Wang, & Ji, 2022). Five organic compounds, including sodium acetate (30 mM), sodium citrate (10 mM), D-glucose (10 mM), D-cellobiose (5 mM), and leucine (10 mM), were added to the medium of the five enrichments, respectively. The total carbon content was 60 mM in each enrichment. Other components of the medium included 0.1 g/L $MgSO_4 \cdot 7H_2O$, 0.05 g/L $CaCl_2$, 1.2 g/L KH_2PO_4, 2.4 g/L Na_2HPO_4, 0.2 g/L NH_4Cl, 20 mM $NaNO_3$, 2 mL trace element solution, and 2 mL vitamin solution (Li, Wang, & Ji, 2022). The cultures were sparged with dinitrogen and sealed with rubber stoppers to maintain the anoxic environment. All incubations were conducted at room temperature in the dark in a shaker. The incubations were passaged 10 times with 20-fold dilution. Each generation lasted for 2 days.

Isotope fractionation experiment of the enrichments

The eleventh generation of the five enrichments was used for the isotope fractionation experiment. Two treatments were set up for each enrichment. The first treatment was conducted with water with isotopes of natural abundance. The second treatment was conducted with ^{18}O-labelled water at a final $\delta^{18}O$ of approximately 100‰ to analyse the back reaction of nitrite (nitrite re-oxidation to nitrate). Each treatment was conducted in triplicated systems. Isotope samples were collected during nitrate reduction with syringes. The filtered culture samples were used for wet chemistry analysis and isotope measurements. Nitrate was measured with an ion chromatograph according to the previous method (Li et al., 2021). Nitrite was measured by a reaction with sulfanilamide and N-(1-naphthyl) ethylenediamine (Bendschneider & Robinson, 1952). Samples for nitrate isotope analysis were added with the sulfamic acid solution immediately after sample collection to remove the effect of nitrite. Any sample with a nitrite/nitrate concentration ratio higher than 7 was not included in the isotope measurement and analysis due to the limitation of the sulfamic acid method (Granger & Sigman, 2009). The complete removal of nitrite in isotope samples was confirmed with the same reaction (Bendschneider & Robinson, 1952).

In situ isotope analysis

A total of 66 water samples were collected from different water depths of Danjiangkou Reservoir (Figure S1) and the surface water of six of its inflowing rivers in July and September of 2018. The water depths of samples were used as a proxy to indicate oxic or hypoxic/anoxic water types (Table S1). Nitrate isotopes were measured in the filtered water samples with the same methods as used for the laboratory-built enrichments.

Isotope measurement and calculation

$\delta^{15}N$ and $\delta^{18}O$ values of nitrate were measured with the denitrifier method (Casciotti et al., 2002; Sigman et al., 2001). During sample preparation, nitrate was reduced to nitrous oxide (N_2O) by a denitrifying bacterium (*Pseudomonas aureofaciens* ATCC 13985), which lacks the nitrous oxide reductase. Water and carbon dioxide in the samples were removed using scrubbers. N_2O was compressed onto a capillary column (PoraPlot Q, 25 m, 0.32 mm id, 10 mm df, Agilent Technologies) at 35°C. $\delta^{15}N$ and $\delta^{18}O$ of the N_2O samples were measured with a trace gas preparation unit (Precon, Finnigan, Germany) coupled to an isotope ratio mass spectrometer (Delta V plus, Finnigan, Germany). $\delta^{15}N$ values were calibrated against air with

USGS32 ($180.0 \pm 1.0‰$), USGS34 ($-1.8 \pm 0.2‰$) and IAEA N3 ($4.7 \pm 0.2‰$). $\delta^{18}O$ values were calibrated against VSMOW (Vienna Standard Mean Ocean Water) with USGS34 ($27.8 \pm 0.4‰$), IAEA N3 ($25.6 \pm 0.4‰$) and USGS35 ($56.8 \pm 0.3‰$).

To analyse the influence of the oxygen atom exchange between nitrite and water, isotopes of water in the laboratory were also measured. High-purity nitrogen was used as the carrier gas and adjusted the pressure to 2.5 psi. Water samples were injected with syringes into the vaporisation chamber. High temperature, fast airflow, and slow liquid water input rate ensured samples to be fully vaporised in the vaporisation chamber. Isotopes of water were measured with a liquid water and water vapour isotope analyser Picarro L1115-I (Picarro Inc. www.picarro.com).

Isotope ratios of N and O atoms were calculated in delta (δ) notation in units of per mil (‰), according to the following equations:

$$\delta^{15}N_{sample} = \left[\left(^{15}N/^{14}N\right)_{sample} \Big/ \left(^{15}N/^{14}N\right)_{reference} - 1 \right] \times 1000‰,$$

$$\delta^{18}O_{sample} = \left[\left(^{18}O/^{16}O\right)_{sample} \Big/ \left(^{18}N/^{16}N\right)_{reference} - 1 \right] \times 1000‰.$$

The $\delta^{15}N_{sample}$ and $\delta^{18}O_{sample}$ values were fit to the following equations to calculate stable isotope enrichment factor ε of $\delta^{15}N$ and $\delta^{18}O$ during nitrate reduction:

$$^{15}\varepsilon = \ln\left[\left(\delta^{15}N + 1\right) \Big/ \left(\delta^{15}N_{initial} + 1\right) \right] \times \ln(f)^{-1} \times 1000‰,$$

$$^{18}\varepsilon = \ln\left[\left(\delta^{18}O + 1\right) \Big/ \left(\delta^{18}O_{initial} + 1\right) \right] \times \ln(f)^{-1} \times 1000‰,$$

$$f = c(NO_3^-)/c(NO_3^-)_{initial},$$

where $c(NO_3^-)$ is the concentration of nitrate in the sample, and $c(NO_3^-)_{initial}$ is the initial concentration of nitrate.

A linear derivation was used to plot $\delta^{15}N$ and $\delta^{18}O$ against $\ln(f)$,

$$\delta^{15}N = \delta^{15}N_{initial} + {}^{15}\varepsilon \times \ln(f),$$

$$\delta^{18}O = \delta^{18}O_{initial} + {}^{18}\varepsilon \times \ln(f).$$

Metagenomic sequencing and enzyme analysis

Metagenomes were collected in each enrichment at the end of the tenth generation. DNA extraction and

sequencing were performed using the same workflow as described in a previous study (Li, Wang, & Ji, 2022). Quality-filtered reads were assembled into contigs with MEGAHIT v1.2.9 (Li et al., 2015). Coverage of the contigs in each metagenome was obtained by first mapping raw reads to the contigs with BBmap v38.18 and then using the "jgi_summarize_bam_contig_depths" script within MetaBat v2:2.15 (Kang et al., 2019). The contigs were subsequently binned into metagenome-assembled-genomes (MAGs) with MetaBat v2:2.15 based on the tetra-nucleotide frequency and coverage information (Kang et al., 2019). Genome characteristics were obtained with CheckM v1.1.3 (Parks et al., 2015). NMDS analysis was performed based on the abundance of MAGs with the "vegan" package in R v4.0.3.

Hidden Markov models downloaded from the TIGR-FAMs database were used to identify and quantify the nitrate reductases: NapA (TIGR01706) and NarG (TIGR01580). The abundance of the two nitrate reductases was quantified in contigs and reads, respectively. For the abundance in contigs, proteins were predicted in contigs by Prodigal (Hyatt et al., 2010) and the nitrate reductases were searched against the obtained proteins. False positives were removed manually. The coverage of the nitrate reductases was normalised by the average coverage of all proteins. For the abundance in reads, the nitrate reductases were searched against all quality-filtered reads with hmmsearch with an e-value cut-off of 1×10^{-5} (Eddy, 2008). To remove false positives, all hit reads were run against the protein database of MetaErg v2.25 (Dong & Strous, 2019) using DIAMOND BLASTX (Buchfink et al., 2015). Only those that were still hit to a nitrate reductase were included, whereas other reads that were hit to another protein were considered false positives. The abundance was calculated with the reads per kilobase of per million reads method.

Metatranscriptomic sequencing and analysis

Metatranscriptomes were collected at the end of the isotope experiments from the enrichments with acetate, cellobiose, and leucine. Total RNAs were extracted using the E.Z.N.A.® Soil RNA Midi Kit (Omega Bio-tek) according to the manufacturer's protocol. RNA concentrations were quantified with a NanoDrop2000 (Thermo Fisher Scientific). RNA quality was examined with the 1% agarose gel electrophoresis system and assessed using an RNA6000 Nano chip (total RNA) in an Agilent 2100 Bioanalyzer. Total RNA was subjected to an rRNA removal procedure using the Ribo-zero Magnetic kit according to the manufacturer's instruction (Epicentre, an Illumina® company). cDNA libraries were constructed using TruSeq™ RNA sample prep kit (Illumina). The barcoded libraries were sequenced on

the Illumina Hiseq 2500 platform using HiSeq 4000 PE Cluster Kit and HiSeq 4000 SBS Kits.

3′ and 5′ ends were stripped using SeqPrep (https://github.com/jstjohn/SeqPrep). Low-quality reads (length < 50 bp or with a quality value <20 or having N bases) were removed by Sickle (https://github.com/najoshi/sickle). SortMeRNA v2.1b was applied to remove ribosomes with an e-value cut-off of 1×10^{-10} (Kopylova et al., 2012). The filtered reads were mapped to the contigs using BBmap v38.18. The expression of the nitrate reductase genes was calculated with filtered reads and contigs using the same methods as described in the metagenomic analysis section.

RESULTS AND DISCUSSION

Nitrate reduction

Experiments were conducted with and without $H_2^{18}O$ for denitrifying enrichments with five different forms of organic carbon as the electron donor. Nitrate and nitrite concentrations were monitored in each replicate (Figures S2 and S3). For the experiments without heavy isotopes, results of the acetate and leucine enrichments were derived from a previous study (Li, Wang, & Ji, 2022). In the enrichment with acetate, 23.1 ± 2.2 mM nitrate was reduced in 53 h with 10.5 ± 3.7 mM nitrite accumulated. Within the same incubation time, 25.8 ± 1.6 mM nitrate was reduced and 9.2 ± 1.3 mM nitrite accumulated in the enrichment with citrate. With glucose, 29.0 ± 0.9 mM nitrate was reduced with 5.8 ± 1.9 mM nitrite accumulated in 85 h. With cellobiose, 26.4 ± 0.9 mM nitrate was reduced and 16.1 ± 0.3 mM nitrite accumulated in 48 h. In the enrichment with leucine, 24.8 ± 1.1 mM nitrate was reduced with 11.4 ± 1.5 mM nitrite accumulated in 51 h. The enrichment with cellobiose showed the highest average nitrate reduction rate, whereas the enrichment with glucose had the lowest.

Enrichment factors of N and O isotopes

N and O isotopes were measured during the time course experiments (Table S2) and plotted against the natural log of the remaining nitrate over initial nitrate (ln (f)) with a linear regression fit to show isotope fractionation factors in each enrichment (Figures 1, S4, and S5). The enrichment with leucine showed a lower δ^{15}N-nitrate enrichment factor ($^{15}ε = -11.6 ± 0.6‰$), whereas other incubations enriched δ^{15}N in similar ranges ($^{15}ε = -18.0 ± 1.1‰$ in the enrichment with citrate, $^{15}ε = -18.6 ± 0.6‰$ in the enrichment with cellobiose, $^{15}ε = -19.5 ± 0.6‰$ in the enrichment with glucose and $^{15}ε = -21.6 ± 0.8‰$ in the enrichment with acetate) (Figure 1A).
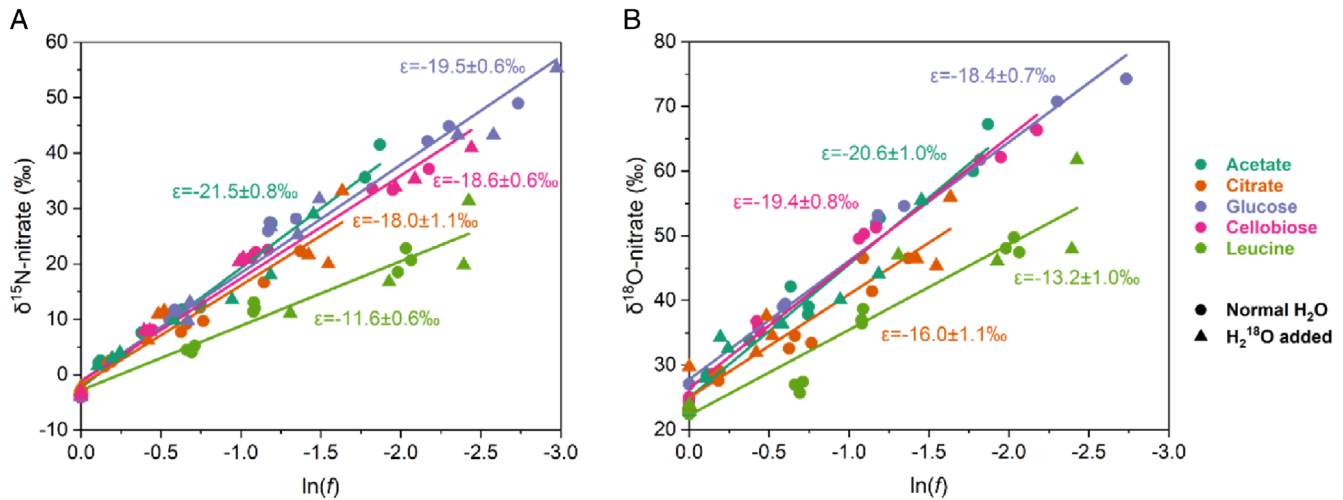
FIGURE 1 (A) δ^{15}N- and (B) δ^{18}O-nitrate versus $\ln(f)$ in the enrichments with acetate, citrate, glucose, cellobiose, and leucine, represented with different colours. Treatments with and without $H_2^{18}O$ are indicated with different shapes.

The oxygen atom of nitrite exchanges with the oxygen atom of water (Casciotti et al., 2007), so oxygen isotope values of nitrate would be influenced if there is nitrite re-oxidised to nitrate. Thus, two treatments were included—one with $H_2^{18}O$ addition and the other without $H_2^{18}O$. For most enrichments, we did not observe significant differences in $^{18}\varepsilon$ between the treatments with and without $H_2^{18}O$ ($p > 0.05$). However, in the enrichment with glucose, the treatment with $H_2^{18}O$ showed significantly higher $^{18}\varepsilon$ values ($^{18}\varepsilon = -28.2 \pm 1.3‰$) than the treatment without $H_2^{18}O$ ($^{18}\varepsilon = -18.5 \pm 0.5‰$, $p = 0.0006$) (Figure S5). Two reasons might explain such a difference, (1) part of nitrite re-oxidised to nitrate during heterotrophic denitrification, (2) nitrite was not removed completely with the sulfamic acid approach (Granger & Sigman, 2009) during the preparation of isotope samples. The first reason was more likely to happen, because we used the same workflow to prepare samples for isotope measurements and other enrichments did not show such a difference. In addition, the enrichment with glucose had the least amount of nitrite accumulation (5.8 ± 1.9 mM nitrite within 85 h) and no sample had a nitrite/nitrate concentration ratio higher than 7, where the sulfamic acid method should be effective enough to remove the impact of nitrite (Granger & Sigman, 2009). The removal of nitrite was confirmed after using sulfamic acid as well (Bendschneider & Robinson, 1952). Thus, part of the nitrite might oxidise to produce nitrate during glucose-dependent denitrification. $\delta^{18}O$ of water we used for the experiment was $-59.3 \pm 0.2‰$, which was lower than any $\delta^{18}O$ values we obtained with nitrate. We only included the treatment without $H_2^{18}O$ in the enrichment with glucose during the analysis (Figure 1B), but the $^{18}\varepsilon$ value ($-18.4 \pm 0.7‰$) might be underestimated considering this issue. The lowest $^{18}\varepsilon$ value still showed in the enrichment with leucine ($^{18}\varepsilon = -13.2 \pm 1.0‰$), while other enrichments had

higher $^{18}\varepsilon$ values ($^{18}\varepsilon = -16.0 \pm 1.1‰$ in the enrichment with citrate, $^{18}\varepsilon = -19.4 \pm 0.8‰$ in the enrichment with cellobiose and $^{18}\varepsilon = -20.6 \pm 1.0‰$ in the enrichment with acetate).

The proportionality of N and O isotopes

The proportionality of N and O isotopes is usually used to indicate microbial nitrate reduction, as the two nitrate reductases induce specific proportionalities (Asamoto et al., 2021). According to previous studies, NapA led to a $^{18}\varepsilon/^{15}\varepsilon$ proportionality of around 0.5 while NarG led to a $^{18}\varepsilon/^{15}\varepsilon$ value of around 1.0 (Asamoto et al., 2021; Frey et al., 2014; Granger et al., 2008; Treibergs & Granger, 2017). In our results, though there was no significant difference in $^{18}\varepsilon$ between the treatments with and without $H_2^{18}O$ in the enrichment with cellobiose, we did observe a higher $^{18}\varepsilon/^{15}\varepsilon$ with $H_2^{18}O$ ($^{18}\varepsilon/^{15}\varepsilon = 1.14 \pm 0.03‰$) than that without $H_2^{18}O$ ($^{18}\varepsilon/^{15}\varepsilon = 1.01 \pm 0.006‰$) (Figure S6). Undoubtedly in the enrichment with glucose, the $^{18}\varepsilon/^{15}\varepsilon$ ratio with $H_2^{18}O$ ($^{18}\varepsilon/^{15}\varepsilon = 1.45 \pm 0.11‰$) was higher than that without $H_2^{18}O$ ($^{18}\varepsilon/^{15}\varepsilon = 0.92 \pm 0.02‰$). The other three enrichments did not have such a difference between the treatments with and without $H_2^{18}O$. Cellobiose and glucose are sugars, whereas acetate and citrate are organic acids, and leucine is an amino acid. There is a possibility that sugars induce nitrite re-oxidation to some extent, while organic acids and amino acids do not. This needs future experiments with more carbon sources from different chemical classes.

$^{18}\varepsilon/^{15}\varepsilon$ might be underestimated in the enrichments with glucose and cellobiose because $\delta^{18}O$-water was lower than any measured $\delta^{18}O$-nitrate values. As part of re-oxidised nitrite was derived from water, this lowered $\delta^{18}O$-nitrate. If we do not consider this issue, the

five carbon sources led to similar $^{18}\varepsilon/^{15}\varepsilon$ values close to 1 with slight variance (Figure 2). We hypothesised that different carbon sources led to different isotopic characteristics. It is true that $^{18}\varepsilon$ and $^{15}\varepsilon$ values changed with carbon sources, but $^{18}\varepsilon/^{15}\varepsilon$ followed the same value. This might be explained by the similarity of enzymes and microorganisms, because the direct factor controlling isotope fractionation in our experiments is the microorganisms or, more specifically, the associated nitrate reductases.

Functional microorganisms with NapA and NarG

Characteristics of the five metagenomes were reported previously (Li, Wang, & Ji, 2022) and 16 MAGs were obtained (Table S3). Acetate mainly enriched *Pseudomonas* 1, whereas leucine enriched *Pseudomonas* 2, *Pseudomonas* 3, and *Burkholderiaceae* 1 (Figure 3).
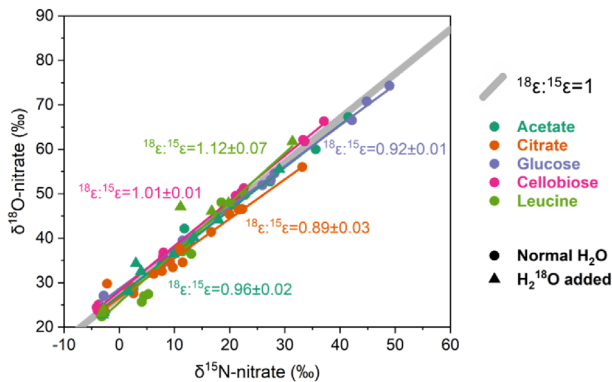

FIGURE 2 δ^{18}O- versus δ^{15}N-nitrate in the enrichments with acetate, citrate, glucose, cellobiose, and leucine represented with different colours. Treatments with and without H_2^{18}O are indicated with different shapes. The grey thick line indicates $^{18}\varepsilon/^{15}\varepsilon = 1$.
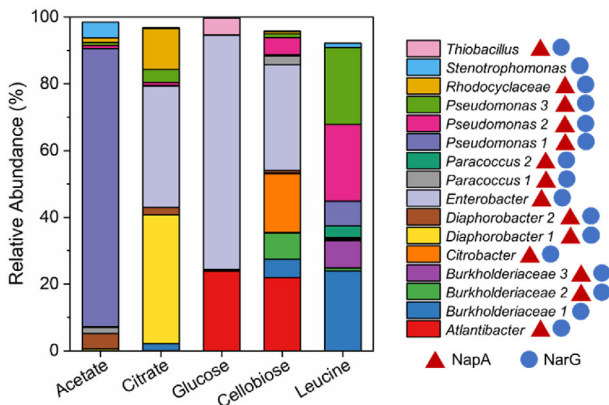

FIGURE 3 Community structure in the five enrichments based on metagenome-assembled-genomes (MAGs) (Li, Wang, & Ji, 2022). The presence of the periplasmic nitrate reductase (NapA) and cytoplasmic nitrate reductase (NarG) is indicated with different colours and shapes alongside each MAG.

The other three carbon sources enriched *Enterobacter*, while glucose and cellobiose enriched *Atlantibacter* in parallel and citrate enriched *Diaphorobacter* 1 as well. More similarity showed between the enrichments with glucose and cellobiose, the two sugars, in regard to microbial populations. All recovered microbial populations contained the cytoplasmic nitrate reductase NarG. Most populations also contained the periplasmic nitrate reductase NapA, with two exceptions—*Burkholderiaceae* 1 and *Stenotrophomonas* did not have a NapA reductase. Though the five enrichments did not assemble similar microbial communities, most of the enriched populations contained both types of nitrate reductases.

Abundance and affiliated microbial taxonomy of nitrate reductases

Nitrate reductase encoding genes *napA* and *narG* were quantified in assembled contigs (Figure 4A). For metagenomes, the enrichment with leucine had the highest abundance of NapA (85.61) and the highest ratio of NapA/NarG (1.84), while the enrichment with cellobiose had the highest abundance of NarG (66.89) and the lowest value of NapA/NarG (0.62). In metatranscriptomes, different patterns occurred—the highest expression of NarG (93.07) appeared in the enrichment with leucine, whereas the lowest NapA/NarG (0.06) still showed in the enrichment with cellobiose but the ratio was much lower than that in the corresponding metagenome. For the enrichment with acetate, similar NapA to NarG abundance, and expression appeared in the metagenome (1.72) and the metatranscriptome (1.47), respectively. The quantification was also conducted at the reading level (Table S4). In general, the NapA/NarG ratios were similar at the contig and read levels for each metagenome/metatranscriptome.

The microbial taxonomy of each enzyme was obtained by searching the enzymes against reference sequences (Figure 4B–E). In metagenomes of the enrichments with acetate and leucine, NapA was more abundant than NarG, and *Pseudomonas*-type NapA was the most abundant nitrate reductase (Figure 4B). They were mainly carried by *Pseudomonas* 1 in the enrichment with acetate, whereas some *Pseudomonas*-type NapA were obtained from unbinned contigs in the enrichment with leucine (Table S5). In the enrichment with citrate, NapA was mainly carried by *Enterobacter* (mainly from the MAG *Enterobacter*), Candidatus *Accumulibacter* (mainly from the MAG *Rhodocyclaceae*), and *Diaphorobacter* (mainly from the MAG *Diaphorobacter* 1). In the enrichments with glucose and cellobiose, abundant NapA reductases belonged to *Enterobacter* and *Atlantibacter*, respectively affiliated with the MAGs *Enterobacter* and *Atlantibacter*.

For the enrichments with citrate, glucose, and cellobiose, NarG was more abundant than NapA and the
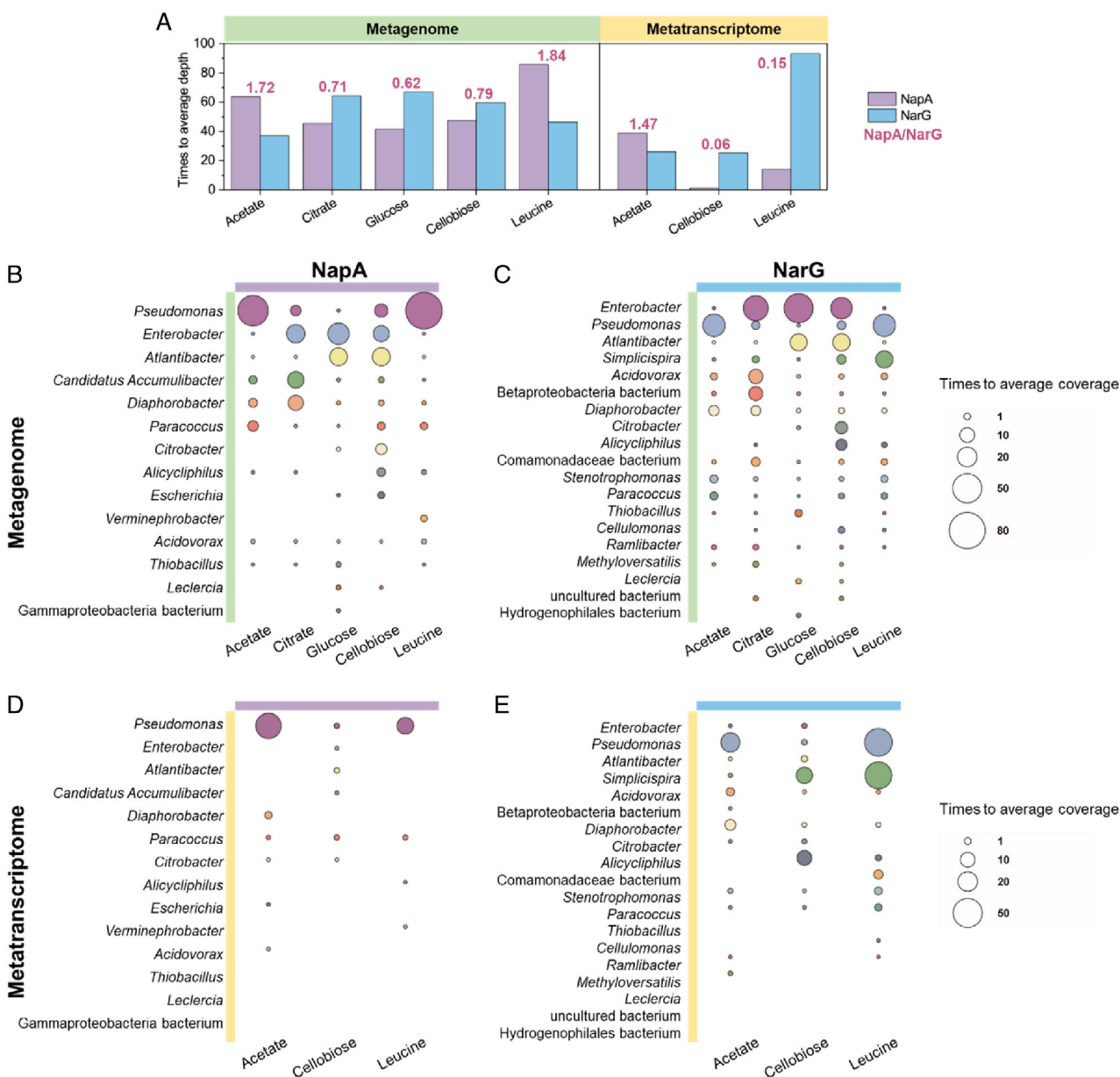
FIGURE 4 (A) Relative sequence abundance of the two nitrate reductases in metagenomes and metatranscriptomes in the enrichments with acetate, citrate, glucose, cellobiose, and leucine. Relative sequence abundance was obtained by normalising the depth of the functional genes by the average depth of all genes. NapA/NarG values are indicated alongside each metagenome/metatranscriptome. (B)–(E) Taxonomy affiliations of (B), (D) NapA and (C), (E) NarG in (B), (C) metagenomes and (D), (E) metatranscriptomes in the enrichments.

most abundant NarG was carried by *Enterobacter* (mainly from the MAG *Enterobacter*) in metagenomes (Figure 4C). The enrichment with citrate also contained abundant NarG carried by the MAG *Diaphorobacter* 1 (Table S6). The second most abundant NarG in the enrichments with glucose and cellobiose was affiliated with *Atlantibacter*. With non-metric multidimensional scaling (NMDS) analysis based on microbial affiliations and abundance of the two nitrate reductases, the distance between the enrichments with glucose and cellobiose was the shortest (Figure S7), suggesting the

presence of similar enzymes which might explain the nitrite re-oxidation phenomenon occurred in both incubations.

For metatranscriptomes, *Pseudomonas*-type NapA was still the most actively expressed nitrate reductase in the enrichment with acetate (Figure 4D). *Pseudomonas*- and *Simplicispira*-type NarG was most active in the enrichment with leucine (Figure 4E). They were partly carried by the MAGs *Pseudomonas* 2, *Pseudomonas* 3, *Burkholderiaceae* 1, and *Burkholderiaceae* 3 (Table S6). The enrichment with cellobiose had less NapA

expressed, while *Simplicispira*- and *Alicycliphilus*-type NarG were expressed actively and they were carried by the MAGs *Burkholderiaceae* 1 and *Burkholderiaceae* 2, respectively.

Mechanisms of the robustness of $^{18}\varepsilon/^{15}\varepsilon$

We observed different abundance and expressions of NapA and NarG in the enrichments. Several environmental factors influence the expression of NapA versus NarG in pure cultures. NapA had a higher affinity for nitrate than NarG (Sparacino-Watkins et al., 2014). Both NapA and NarG are transcribed in anoxic environments, while only NapA operates in hypoxic environments but it is attributed to the assimilation by cell growth under such conditions (Kuypers et al., 2018; Lin et al., 2018; Sears et al., 1997; Sears et al., 2000). NapA was more highly transcribed with the availability of reduced carbon sources (Sears et al., 1997; Sears et al., 2000). In our study, nitrate concentration was limited in all enrichments, and leucine was the only reduced carbon source. Though the highest abundance of NapA in metagenomes was indeed observed in the enrichment with leucine, it was much less expressed than NarG in the metatranscriptome. Compared to previously reported findings with isolated strains, we did not observe a consistent pattern of the abundance/expression of NapA versus NarG under the control of carbon sources. In the denitrifying system, the situation might be that carbon sources influence the selection of specific populations (Carlson et al., 2020; Flynn et al., 2017; Goldfarb et al., 2011; Goldford et al., 2018; Wawrik et al., 2005), which contain NapA and/or NarG. For example, glucose favours the enrichment of Enterobacteriaceae populations, while organic acids favour Pseudomonadaceae (Carlson et al., 2020; Goldford et al., 2018). These seem to be more consistent with our results—acetate highly enriched *Pseudomonas*, while glucose enriched *Enterobacter*, and the two populations contained both NapA and NarG (Figure 3).

Nevertheless, despite the different abundance and expression of NapA and NarG, $^{18}\varepsilon/^{15}\varepsilon$ was always around 1 (Figure 2). This discovery is surprising and conflicting with the current knowledge that $^{18}\varepsilon/^{15}\varepsilon$ equals 0.5 during the operation of NapA, and 1.0 during the operation of NarG (Asamoto et al., 2021; Frey et al., 2014; Granger et al., 2008; Treibergs & Granger, 2017). Truly NarG was more highly expressed than NapA in the enrichments with cellobiose and leucine. The conflict mainly existed in the enrichment with acetate—though NapA was expressed comparably to NarG, $\delta^{18}O$- and $\delta^{15}N$-nitrate still followed 1. Two reasons might explain the situation. First, our knowledge of isotope fractionation characteristics of the enzyme is still limited. For example, *Bacillus*-type NarG is an exception of common NarG reductases and it showed

a $^{18}\varepsilon/^{15}\varepsilon$ value near 0.6 (Asamoto et al., 2021). A very distinct isotope effect of NapA was also reported with Rhodocyclales, though it was not based on pure cultures (Li, Diao, Wang, et al., 2022). There is a possibility that the expressed NapA reductases conduct nitrate reduction with a $^{18}\varepsilon/^{15}\varepsilon$ proportionality of 1.0. The second possible reason is that though NapA was transcribed with acetate, it may not participate in nitrate reduction. Previous findings suggested NapA could function in other biochemical processes such as the reduction of vanadium and magnetite biomineralisation (He et al., 2021; Li et al., 2012). Even if these were unlikely to happen in the denitrifying enrichments, it indicates we know little about the real role of NapA.

The most highly expressed NapA was affiliated with *Pseudomonas* in the enrichment with acetate. Previous studies analysed isotope fractionation characteristics of several *Pseudomonas* strains, including *P. denitrificans* (Asamoto et al., 2021; Treibergs & Granger, 2017), *P. aeruginosa* (Asamoto et al., 2021) and *P. chlororaphis* (Granger et al., 2008). All of them contain both NapA and NarG and showed a $^{18}\varepsilon/^{15}\varepsilon$ value of around 1.0 during nitrate reduction (Asamoto et al., 2021; Granger et al., 2008; Treibergs & Granger, 2017). With the gene deletion experiment, $^{18}\varepsilon/^{15}\varepsilon$ was around 1.0 if NapA was knocked out and around 0.5 if the NarG was deleted (Asamoto et al., 2021). Such a phenomenon seems to indicate when NarG is present, the expression of NapA is inhibited or NapA does not participate in nitrate reduction. However, molecular evidence is missing as there was no transcriptomic or proteomic data in the studies. Therefore, we could not draw conclusions on which explanation is more likely. Further experiments should investigate whether NapA is expressed and what NapA is actually doing during nitrate reduction in a bacterium with both NapA and NarG. More advanced technologies such as single-cell sequencing and visualisation may help to provide the answer at the cell level.

Extension to environmental study

Our hypothesis was falsified as nitrate reduction always fractionated N and O following a proportionality around unity in all enrichments, though $^{15}\varepsilon$ and $^{18}\varepsilon$ varied with carbon sources. This provides an opportunity to accurately determine heterotrophic denitrification in aquatic environments with stable isotope analysis.

Isotopic values of nitrate were measured for 66 water samples collected from Danjiangkou Reservoir, the biggest reservoir in China (1023 km^2) with the deepest water depth of around 80 m (Figure 5). Samples from the surface water (about 0.5 m) were considered to be oxic, whereas samples collected from waters below 12 m were considered hypoxic or anoxic (Table S1). Overall, we did not observe a clear
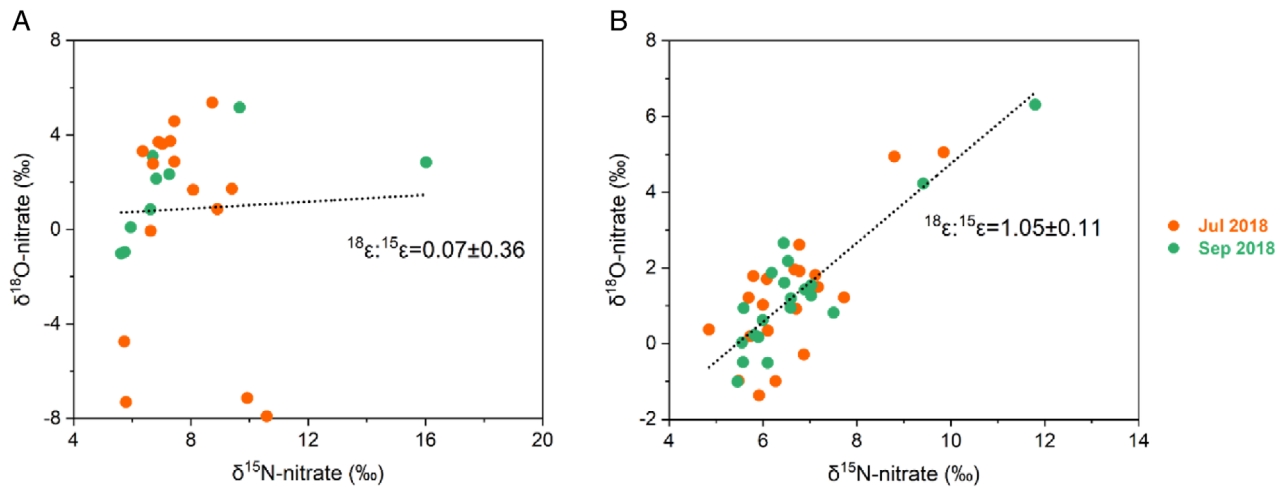
FIGURE 5 δ^{18}O- versus δ^{15}N-nitrate in samples collected from (A) the surface water (around 0.5 m) and (B) the deep waters ($\geq$ 12 m) of Danjiangkou Reservoir.

correlation between δ^{15}N- and δ^{18}O-nitrate in oxic samples (Figure 5A), but $^{18}\varepsilon/^{15}\varepsilon$ was 1.05 ± 0.11 in hypoxic/anoxic samples (Figure 5B), which matched exactly to the observed pattern of heterotrophic denitrification in our enrichments. In oxic areas, both nitrification and aerobic denitrification were active and controlled the fractionation of nitrate isotopes. In deeper waters, oxygen becomes less available, which limited the activity of nitrifying microorganisms and provided a favourable niche for denitrifiers, and a clear pattern of nitrate isotopes emerged.

According to previous studies, δ^{18}O/δ^{15}N ratios vary between 0.5 and 0.7 in terrestrial/freshwater systems, whereas δ^{18}O/δ^{15}N ratios normally fall into the range of 0.9 to 1.0 in marine systems (Asamoto et al., 2021; Kendall et al., 2007). This difference was inferred to be introduced by different expressions of NapA and NarG—NapA was more important in freshwaters, while NarG was more important in oceans (Asamoto et al., 2021). However, in situ molecular data showed that the abundance of NarG was comparable to or even higher than NapA not only in marine systems but also in freshwater lakes (Bru et al., 2007; Fan et al., 2019; Melton et al., 2014; Schaedler et al., 2018), rivers (Bru et al., 2007; Correa-Galeote et al., 2017; Li et al., 2020; Shen et al., 2019) and groundwaters (Bru et al., 2007; Petelet-Giraud et al., 2021). Therefore, the abundances of NapA versus NarG seem not to be able to explain different nitrate isotope patterns in oceans and freshwaters. Here, we suggested the difference might be induced by other processes such as nitrification. In Danjiangkou Reservoir, though we did not observe a clear pattern between nitrogen and oxygen isotopes of nitrate in shallow waters, δ^{18}O- versus δ^{15}N-nitrate showed a linear proportionality around 1 in deep waters (Figure 5). A previous study also suggested that the difference in δ^{18}O-/δ^{15}N-nitrate ratios between marine and freshwater systems resulted from the activity of nitrification and anammox (Granger & Wankel, 2016). Nitrification disrupts the isotopic pattern of denitrification in oxic areas, which greatly changes the interpretation of nitrate isotopic records in samples collected from shallow waters (Carrey et al., 2021; Fang et al., 2015; Paredes et al., 2020; Torres-Martinez et al., 2020; Wexler et al., 2014; Yi et al., 2017). Meanwhile, the $^{18}\varepsilon/^{15}\varepsilon$ value around 1 is still a robust indicator for the first step of heterotrophic denitrification, independent from the change in carbon sources in denitrifying environments.

CONCLUSIONS

Five denitrifying enrichments were inoculated with freshwater samples and incubated with different organic carbon sources. The enrichment factors of N- and O-nitrate isotopes were different during denitrification in the five enrichments. However, $^{18}\varepsilon/^{15}\varepsilon$ of nitrate always followed 1 despite the change in carbon sources. Genome-centred metagenomics and metatranscriptomics indicated most enriched denitrifiers had both NapA- and NarG-type nitrate reductases, but they were transcribed to different levels in the five enrichments. In situ measurements of nitrate isotopes in Danjiangkou Reservoir showed $^{18}\varepsilon/^{15}\varepsilon$ followed 1.05 ± 011 in deep waters, but such proportionality did not appear in shallow waters. The results revealed a specific isotope signal of heterotrophic denitrification and had important implications for the understanding of isotope records in aquatic environments.

AUTHOR CONTRIBUTIONS
Shengjie Li: Conceptualization (lead); data curation (equal); formal analysis (lead); investigation (equal); methodology (lead); visualization (lead); writing – original draft (lead); writing – review and editing (equal).

Zhongxin Luo: Data curation (equal); investigation (equal). **Shuo Wang:** Methodology (equal). **Qiong Nan:** Formal analysis (equal). **Guodong ji:** Conceptualization (equal); funding acquisition (lead); methodology (equal); project administration (lead); supervision (lead); writing – review and editing (equal).

ACKNOWLEDGEMENTS

CONFLICT OF INTEREST STATEMENT

The authors declare no conflicts of interest.

DATA AVAILABILITY STATEMENT

All sequences of this study, including the metagenomes and the MAGs, are available at NCBI (PRJNA817706). The Biosamples for the metagenome reads are SAMN26806341—SAMN26806345. The Biosamples for the metatranscriptome reads are SAMN32424859—SAMN32424861. The Biosamples for the MAGs are SAMN26806346—SAMN26806361.

ORCID

Guodong Ji https://orcid.org/0000-0002-0195-2367

REFERENCES

Asamoto, C.K., Rempfert, K.R., Luu, V.H., Younkin, A.D. & Kopf, S.H. (2021) Enzyme-specific coupling of oxygen and nitrogen isotope fractionation of the Nap and Nar nitrate reductases. *Environmental Science and Technology*, 55(8), 5537–5546.

Bauersachs, T., Schouten, S., Compaoré, J., Wollenzien, U., Stal, L.J. & Sinninghe Damsteé, J.S. (2009) Nitrogen isotopic fractionation associated with growth on dinitrogen gas and nitrate by cyanobacteria. *Limnology and Oceanography*, 54(4), 1403–1411.

Bendschneider, K. & Robinson, R. (1952) A new spectrophotometric method for the determination of nitrite in sea water. *Journal of Marine Research*, 11, 87–96.

Bru, D., Sarr, A. & Philippot, L. (2007) Relative abundances of proteobacterial membrane-bound and periplasmic nitrate reductases in selected environments. *Applied and Environmental Microbiology*, 73(18), 5971–5974.

Buchfink, B., Xie, C. & Huson, D.H. (2015) Fast and sensitive protein alignment using DIAMOND. *Nature Methods*, 12(1), 59–60.

Buchwald, C. & Casciotti, K.L. (2010) Oxygen isotopic fractionation and exchange during bacterial nitrite oxidation. *Limnology and Oceanography*, 55(3), 1064–1074.

Canfield, D.E., Glazer, A.N. & Falkowski, P.G. (2010) The evolution and future of Earth's nitrogen cycle. *Science*, 330(6001), 192–196.

Carlson, H.K., Lui, L.M., Price, M.N., Kazakov, A.E., Carr, A.V., Kuehl, J.V. et al. (2020) Selective carbon sources influence the end products of microbial nitrate respiration. *The ISME Journal*, 14(8), 2034–2045.

Carpenter, E.J., Harvey, H.R., Fry, B. & Capone, D.G. (1997) Biogeochemical tracers of the marine cyanobacterium Trichodesmium. *Deep Sea Research Part I: Oceanographic Research Papers*, 44(1), 27–38.

Carrey, R., Ballesté, E., Blanch, A.R., Lucena, F., Pons, P., López, J.M. et al. (2021) Combining multi-isotopic and molecular source tracking methods to identify nitrate pollution sources in surface and groundwater. *Water Research*, 188, 116537.

Casciotti, K.L. (2009) Inverse kinetic isotope fractionation during bacterial nitrite oxidation. *Geochimica et Cosmochimica Acta*, 73(7), 2061–2076.

Casciotti, K.L., Bohlke, J.K., McIlvin, M.R., Mroczkowski, S.J. & Hannon, J.E. (2007) Oxygen isotopes in nitrite: analysis, calibration, and equilibration. *Analytical Chemistry*, 79(6), 2427–2436.

Casciotti, K.L., Sigman, D.M., Hastings, M.G., Bohlke, J.K. & Hilkert, A. (2002) Measurement of the oxygen isotopic composition of nitrate in seawater and freshwater using the denitrifier method. *Analytical Chemistry*, 74(19), 4905–4912.

Correa-Galeote, D., Tortosa, G., Moreno, S., Bru, D., Philippot, L. & Bedmar, E.J. (2017) Spatio-temporal variations in the abundance and structure of denitrifier communities in sediments differing in nitrate content. *Current Issues in Molecular Biology*, 24, 71–102.

Dong, X. & Strous, M. (2019) An integrated pipeline for annotation and visualization of metagenomic contigs. *Frontiers in Genetics*, 10, 999.

Eddy, S.R. (2008) A probabilistic model of local sequence alignment that simplifies statistical significance estimation. *PLoS Computational Biology*, 4(5), e1000069.

Fan, Y.Y., Li, B.B., Yang, Z.C., Cheng, Y.Y., Liu, D.F. & Yu, H.Q. (2019) Mediation of functional gene and bacterial community profiles in the sediments of eutrophic Chaohu Lake by total nitrogen and season. *Environmental Pollution*, 250, 233–240.

Fang, Y., Koba, K., Makabe, A., Takahashi, C., Zhu, W., Hayashi, T. et al. (2015) Microbial denitrification dominates nitrate losses from forest ecosystems. *Proceedings of the National Academy of Sciences of the United States of America*, 112(5), 1470–1474.

Fenech, C., Rock, L., Nolan, K., Tobin, J. & Morrissey, A. (2012) The potential for a suite of isotope and chemical markers to differentiate sources of nitrate contamination: a review. *Water Research*, 46(7), 2023–2041.

Flynn, T.M., Koval, J.C., Greenwald, S.M., Owens, S.M., Kemner, K.M. & Antonopoulos, D.A. (2017) Parallelized, aerobic, single carbon-source enrichments from different natural environments contain divergent microbial communities. *Frontiers in Microbiology*, 8, 2321.

Fowler, D., Coyle, M., Skiba, U., Sutton, M.A., Cape, J.N., Reis, S. et al. (2013) The global nitrogen cycle in the twenty-first century. *Philosophical Transactions of the Royal Society B—Biological Sciences*, 368(1621), 20130164.

Frey, C., Hietanen, S., Jurgens, K., Labrenz, M. & Voss, M. (2014) N and O isotope fractionation in nitrate during chemolithoautotrophic denitrification by Sulfurimonas gotlandica. *Environmental Science and Technology*, 48(22), 13229–13237.

Goldfarb, K.C., Karaoz, U., Hanson, C.A., Santee, C.A., Bradford, M.A., Treseder, K.K. et al. (2011) Differential growth responses of soil bacterial taxa to carbon substrates of varying chemical recalcitrance. *Frontiers in Microbiology*, 2, 94.

Goldford, J.E., Lu, N., Bajic, D., Estrela, S., Tikhonov, M., Sanchez-Gorostiaga, A. et al. (2018) Emergent simplicity in microbial community assembly. *Science*, 361(6401), 469–474.

Granger, J. & Sigman, D.M. (2009) Removal of nitrite with sulfamic acid for nitrate N and O isotope analysis with the denitrifier method. *Rapid Communications in Mass Spectrometry*, 23(23), 3753–3762.

Granger, J., Sigman, D.M., Lehmann, M.F. & Tortell, P.D. (2008) Nitrogen and oxygen isotope fractionation during dissimilatory nitrate reduction by denitrifying bacteria. *Limnology and Oceanography*, 53(6), 2533–2545.

Granger, J. & Wankel, S.D. (2016) Isotopic overprinting of nitrification on denitrification as a ubiquitous and unifying feature of environmental nitrogen cycling. *Proceedings of the National Academy of Sciences of the United States of America*, 113(42), E6391–E6400.

Gruber, N. & Galloway, J.N. (2008) An earth-system perspective of the global nitrogen cycle. *Nature*, 451(7176), 293–296.

He, C., Zhang, B., Lu, J. & Qiu, R. (2021) A newly discovered function of nitrate reductase in chemoautotrophic vanadate transformation by natural mackinawite in aquifer. *Water Research*, 189, 116664.

Hyatt, D., Chen, G.L., Locascio, P.F., Land, M.L., Larimer, F.W. & Hauser, L.J. (2010) Prodigal: prokaryotic gene recognition and translation initiation site identification. *BMC Bioinformatics*, 11, 119.

Kang, D.D., Li, F., Kirton, E., Thomas, A., Egan, R., An, H. et al. (2019) MetaBAT 2: an adaptive binning algorithm for robust and efficient genome reconstruction from metagenome assemblies. *PeerJ*, 7, e7359.

Kendall, C., Elliott, E.M. & Wankel, S.D. (2007) Tracing anthropogenic inputs of nitrogen to ecosystems. In: *Tracing anthropogenic inputs of nitrogen to ecosystems*. Malden, MA: Blackwell.

Kopylova, E., Noe, L. & Touzet, H. (2012) SortMeRNA: fast and accurate filtering of ribosomal RNAs in metatranscriptomic data. *Bioinformatics*, 28(24), 3211–3217.

Kuypers, M.M.M., Marchant, H.K. & Kartal, B. (2018) The microbial nitrogen-cycling network. *Nature Reviews Microbiology*, 16(5), 263–276.

Li, D., Liu, C.M., Luo, R., Sadakane, K. & Lam, T.W. (2015) MEGA-HIT: an ultra-fast single-node solution for large and complex metagenomics assembly via succinct de Bruijn graph. *Bioinformatics*, 31(10), 1674–1676.

Li, M., Li, R., Gao, Y., Resch, C.T., Qian, W.-J., Shi, T. et al. (2020) Nitrate bioreduction dynamics in hyporheic zone sediments under cyclic changes of chemical compositions. *Journal of Hydrology*, 585, 124836.

Li, S., Diao, M., Wang, S., Zhu, X., Dong, X., Strous, M. et al. (2022) Distinct oxygen isotope fractionations driven by different electron donors during microbial nitrate reduction in lake sediments. *Environmental Microbiology Reports*, 14(5), 812–821.

Li, S., Pang, Y. & Ji, G. (2021) Increase of N_2O production during nitrate reduction after long-term sulfide addition in lake sediment microcosms. *Environmental Pollution*, 291, 118231.

Li, S., Wang, S. & Ji, G. (2022) Influences of carbon sources on N_2O production during denitrification in freshwaters: activity, isotopes and functional microbes. *Water Research*, 226, 119315.

Li, S., Wang, S., Pang, Y. & Ji, G. (2022) Influence of electron donors (Fe, C, S) on N_2O production during nitrate reduction in lake sediments: evidence from isotopes and functional genes. *ACS ES&T Water*, 2(7), 1254–1264.

Li, Y., Katzmann, E., Borg, S. & Schuler, D. (2012) The periplasmic nitrate reductase nap is required for anaerobic growth and involved in redox control of magnetite biomineralization in *Magnetospirillum gryphiswaldense*. *Journal of Bacteriology*, 194(18), 4847–4856.

Lin, Y.C., Sekedat, M.D., Cornell, W.C., Silva, G.M., Okegbe, C., Price-Whelan, A. et al. (2018) Phenazines regulate Nap-dependent denitrification in *Pseudomonas aeruginosa* biofilms. *Journal of Bacteriology*, 200(9), e00031.

Macko, S.A., Fogel, M.L., Hare, P.E. & Hoering, T.C. (1987) Isotopic fractionation of nitrogen and carbon in the synthesis of amino acids by microorganisms. *Chemical Geology: Isotope Geoscience Section*, 65(1), 79–92.

Martin, T.S. & Casciotti, K.L. (2016) Nitrogen and oxygen isotopic fractionation during microbial nitrite reduction. *Limnology and Oceanography*, 61(3), 1134–1143.

Melton, E.D., Stief, P., Behrens, S., Kappler, A. & Schmidt, C. (2014) High spatial resolution of distribution and interconnections between Fe- and N-redox processes in profundal lake sediments. *Environmental Microbiology*, 16(10), 3287–3303.

Minagawa, M. & Wada, E. (1986) Nitrogen isotope ratios of red tide organisms in the East China Sea: a characterization of biological nitrogen fixation. *Marine Chemistry*, 19(3), 245–259.

Paredes, I., Otero, N., Soler, A., Green, A.J. & Soto, D.X. (2020) Agricultural and urban delivered nitrate pollution input to Mediterranean temporary freshwaters. *Agriculture, Ecosystems and Environment*, 294, 106859.

Parks, D.H., Imelfort, M., Skennerton, C.T., Hugenholtz, P. & Tyson, G.W. (2015) CheckM: assessing the quality of microbial genomes recovered from isolates, single cells, and metagenomes. *Genome Research*, 25(7), 1043–1055.

Petelet-Giraud, E., Baran, N., Vergnaud-Ayraud, V., Portal, A., Michel, C., Joulian, C. et al. (2021) Elucidating heterogeneous nitrate contamination in a small basement aquifer. A multidisciplinary approach: NO_3 isotopes, CFCs-SF6, microbiological activity, geophysics and hydrogeology. *Journal of Contaminant Hydrology*, 241, 103813.

Richardson, D.J., Berks, B.C., Russell, D.A., Spiro, S. & Taylor, C.J. (2001) Functional, biochemical and genetic diversity of prokaryotic nitrate reductases. *Cellular and Molecular Life Sciences*, 58(2), 165–178.

Robertson, G.P. & Vitousek, P.M. (2009) Nitrogen in agriculture: balancing the cost of an essential resource. *Annual Review of Environment and Resources*, 34(1), 97–125.

Robinson, D. (2001) $\delta^{15}N$ as an integrator of the nitrogen cycle. *Trends in Ecology and Evolution*, 16(3), 153–162.

Schaedler, F., Lockwood, C., Lueder, U., Glombitza, C., Kappler, A. & Schmidt, C. (2018) Microbially mediated coupling of Fe and N cycles by nitrate-reducing Fe(II)-oxidizing bacteria in littoral freshwater sediments. *Applied and Environmental Microbiology*, 84(2), e02013-17.

Sears, H.J., Sawers, G., Berks, B.C., Ferguson, S.J. & Richardson, D.J. (2000) Control of periplasmic nitrate reductase gene expression (napEDABC) from *Paracoccus pantotrophus* in response to oxygen and carbon substrates. *Microbiology*, 146, 2977–2985.

Sears, H.J., Spiro, S. & Richardson, D.J. (1997) Effect of carbon substrate and aeration on nitrate reduction and expression of the periplasmic and membrane-bound nitrate reductases in carbon-limited continuous cultures of *Paracoccus denitrificans* Pd1222. *Microbiology*, 143(12), 3767–3774.

Shen, L., Ouyang, L., Zhu, Y. & Trimmer, M. (2019) Spatial separation of anaerobic ammonium oxidation and nitrite-dependent anaerobic methane oxidation in permeable riverbeds. *Environmental Microbiology*, 21(4), 1185–1195.

Sigman, D.M., Casciotti, K.L., Andreani, M., Barford, C., Galanter, M. & Bohlke, J.K. (2001) A bacterial method for the nitrogen isotopic analysis of nitrate in seawater and freshwater. *Analytical Chemistry*, 73(17), 4145–4153.

Sparacino-Watkins, C., Stolz, J.F. & Basu, P. (2014) Nitrate and periplasmic nitrate reductases. *Chemical Society Reviews*, 43(2), 676–706.

Torres-Martinez, J.A., Mora, A., Knappett, P.S.K., Ornelas-Soto, N. & Mahlknecht, J. (2020) Tracking nitrate and sulfate sources in groundwater of an urbanized valley using a multi-tracer approach combined with a Bayesian isotope mixing model. *Water Research*, 182, 115962.

Treibergs, L.A. & Granger, J. (2017) Enzyme level N and O isotope effects of assimilatory and dissimilatory nitrate reduction. *Limnology and Oceanography*, 62(1), 272–288.

Wawrik, B., Kerkhof, L., Kukor, J. & Zylstra, G. (2005) Effect of different carbon sources on community composition of bacterial enrichments from soil. *Applied and Environmental Microbiology*, 71(11), 6776–6783.

Wexler, S.K., Goodale, C.L., McGuire, K.J., Bailey, S.W. & Groffman, P.M. (2014) Isotopic signals of summer denitrification in a northern hardwood forested catchment. *Proceedings of the National Academy of Sciences of the United States of America*, 111(46), 16413–16418.

Wunderlich, A., Meckenstock, R. & Einsiedl, F. (2012) Effect of different carbon substrates on nitrate stable isotope fractionation during microbial denitrification. *Environmental Science and Technology*, 46(9), 4861–4868.

Xue, D., Botte, J., De Baets, B., Accoe, F., Nestler, A., Taylor, P. et al. (2009) Present limitations and future prospects of stable isotope methods for nitrate source identification in surface- and groundwater. *Water Research*, 43(5), 1159–1170.

Yi, Q., Chen, Q., Hu, L. & Shi, W. (2017) Tracking nitrogen sources, transformation, and transport at a basin scale with complex plain river networks. *Environmental Science and Technology*, 51(10), 5396–5403.

SUPPORTING INFORMATION

Additional supporting information can be found online in the Supporting Information section at the end of this article.